Dissolution, Cements, Sulfides and Bitumen

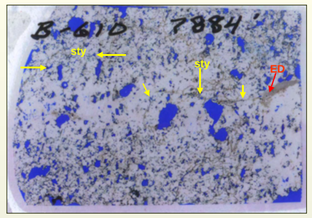

Entire thin section overview showing a completely dolomitized crinoidal grainstone (in white) that has experienced considerable dissolution porosity (in blue). Note that the replacement dolomitization and dissolution cuts across (post-dates) burial related stylolites (see arrows and "sty"). (Well B-610, 7,884 ft., Ø= 9.7%, k = 121 mD. White Card technique. Width of thin section is 2.5 cm.)

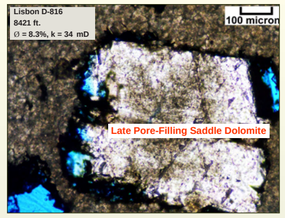

Thin section photomicrograph under plane light showing a saddle dolomite cement that is filling a large pore (either a grain mold or small vug). The dolomite cement has been surrounded by a coating of pyrobitumen (in black). It appears that this late dolomite cement has been partially dissolved or corroded around its margins after the bitumen coating.

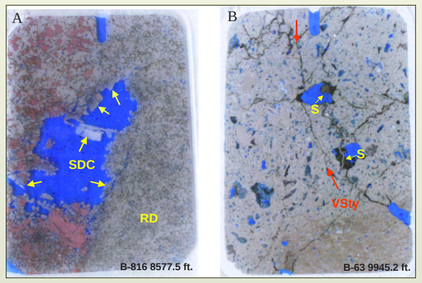

A. Entire thin section overview showing a large dissolution pore (vug) that is lined with saddle dolomite cements (SDC and arrows). The rock matrix consists of rhombic dolomite (RD). Porosity can be seen in the blue colors. (Well B-816, 8,577.5 ft., Ø = 9.8%, k = 1.8 mD. White Card technique. Width of thin section is 2.5 cm.)

B. Entire thin section overview of dolomite that has experienced significant amounts of late dissolution. The brownish areas at the base of the slide are remnants of early, very finely crystalline dolomite. The remaining white areas are much coarser late dolomites and some late calcite. Dissolution of both types of dolomite has resulted in solution-enlarged molds and small vugs (in blue). In addition, there is dissolution along vertical stylolites ("VSty" and red arrows) and fractures. The dissolution event post-dates all of the stylolite and fracture generations in this dolomite. Sulfide minerals (S) are precipitated within some of the pores. (Well B-63, 9,945.2 ft., Ø = 9.8%, k = 1.8 mD. White Card technique. Width of thin section is 2.5 cm.)

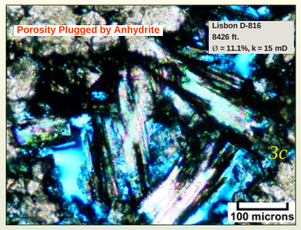

Thin section photomicrograph under cross-polarized light showing lathes of late anhydrite cement (in pastel colors) filling a dissolution pore. The unfilled portions of the pore are seen in the blue areas.

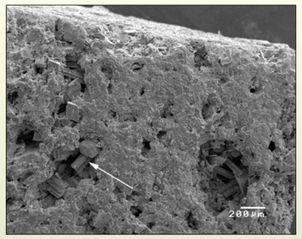

SEM of a core chip of dolomite with molds and small vugs with anhdyrite cements (arrow) in many of the dissolution pores. (Well D-816, 8,426 ft., Ø = 11.1%, k = 15 mD.)

SEM closeup of the lower left portion of the same sample shown in the micrograph to the immediate left. Note the anhydrite cement lathes partially filling a small dissolution vug.

Euhedral Quartz

Large euhedral quartz crystal showing oriented small anhydrite crystals encapsulated in the quartz. The rock matrix surrounding the quartz is rhombic dolomite. (Well D-616, 8,356 ft. Width of image is 1.3 mm.)

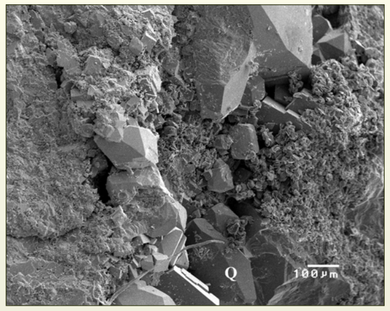

SEM of a core chip containing large, euhedral quartz void fillings (Q) within late dissolution pores. This is the same quartz containing anhydrite inclusions shown in the photomicrograph to the left. The rock matrix consists of dolomite and the black areas are open pores. (Well D-616, 8,356 ft.)

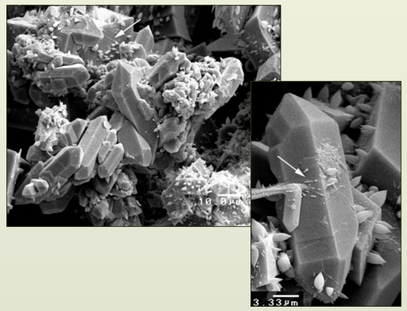

SEM of a core chip showing clusters of euhedral, doubly terminated quartz crystals ("miniherkimers"). The small spiky materials precipitated on many of the surfaces are either pyrobitumens or sulfide minerals. (Well B-816, 8,486 ft.)

SEM showing a closeup of a typical doubly terminated quartz crystal. The linear features (arrow) and the spiky materials on many of the crystal surfaces are composed of either pyrobitumen or sulfide minerals. (Well B-816, 8,486 ft.)

Late Calcite Spar and Bitumen

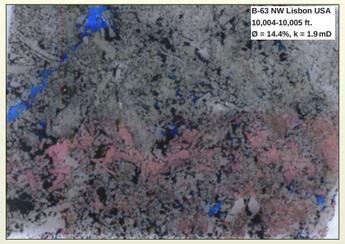

Entire thin section overview of a typical skeletal calcarenite that has been replaced by dolomite. Much of this dolomite is coarsely crystalline with rhombic and saddle habits. Most of the coarse dolomites have been coated with black pyrobitumen. Note that there are multiple stages of dolomite dissolution. One generation of leaching has been partially filled with late calcite spar cement (in red). Additional dissolution along fractures and stylolites can be seen in the blue areas. Width of thin section is 2.5 cm.

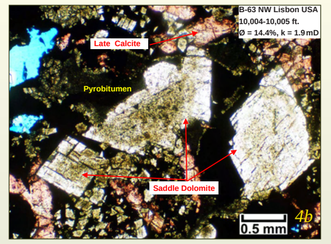

Thin section photomicrograph under plane light from the same sample shown to the left. Note the coarse rhombic and saddle replacement dolomites that display cloudy cores and clear rims. Dissolution pores are filled with pyrobitumen (black) and late calcite spar (red). An additional episode of dissolution can be seen as the open (blue) pores that appear to post-date most of the pyrobitumen emplacement.

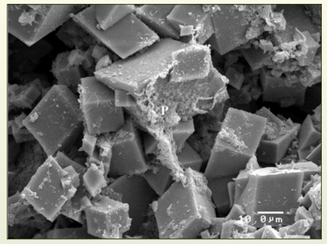

SEM of a core plug showing probable pyrobitumen (P) coating the rhombic dolomite crystal in the center. Pyrobitumen coats many of the other dolomite crystals as well. (Well B-610, 7,886 ft. Ø = 13.8%, k = 114 mD.)

Influence of Faulting

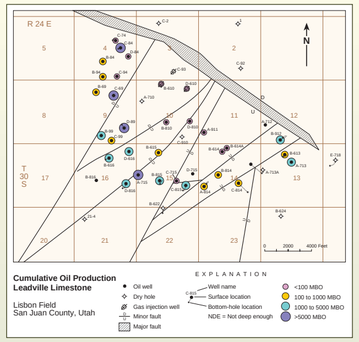

"Bubble map" of cumulative oil production for each well in Lisbon field. Most of the oil production has occurred around a curvilinear fairway because of the gas cap on this field. Note that some of the best performing wells in the field lie on or very close to mapped faults within the field. Some of these faults may have been conduits for fluids that dolomitized and caused dissolution within the original Leadville Limestone. (Gas production from the field has not been accurately gauged, and is not shown on this map.)

Bottom Hole Temperature map for each well in Lisbon field. Despite the inaccuracies associated with BHT measurements in these wells that are mostly from the early 1960's, it is interesting to note that some of the highest measured temperatures (see red circles) are in wells near mapped faults within the field. There may be some elevated residual heat flow along some of these faults today.

Stable Isotopes

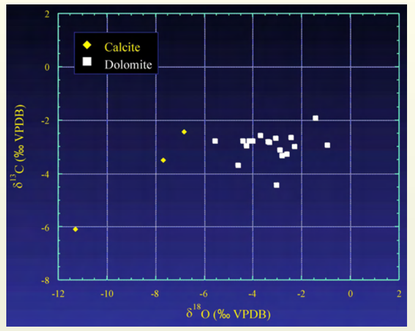

Stable oxygen isotope analyses of dolomites show a linear trend with a fairly narrow range of carbon isotope values.

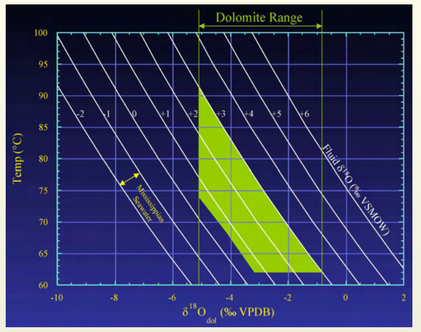

Dolomitzing fluid compositions with respect to del O^{18} are thought to be heavier than normal Mississippian sea water (bracketed by the yellow arrows on the right graph). The green field on the right figure shows our estimate of del O^{18} of dolomitizing fluids at between 0.5 and 3.0‰. Precipitation temperatures were up to ~90°C.

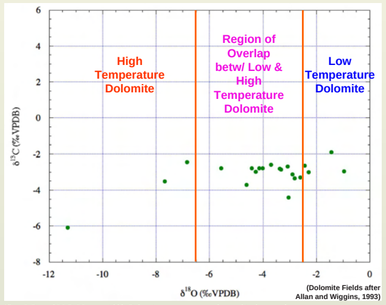

Cross plot of the same del ^{13}C/del O^{18} Leadville data from Lisbon field with the regions of dolomite temperatures of formation suggested by Allan and Wiggins (1993). These fields were defined based upon interpretation of many ancient dolomites by these authors. Note that most of the Leadville data points plot in the region that Allan and Wiggins have called the "overlap of low and high temperature dolomites".

Allan, J. R. and W. D. Wiggins, 1993, Dolomite reservoirs – geochemical techniques for evaluating origin and distribution: Tulsa, OK, AAPG Short Course Note Series No. 36, 129 p.

Dolomite-Water Equilibrium

- Mississippian seawater was in the range of -2 to -1‰ (Veizer et al., 1999)
- Leadville reflux dolomitization likely from evaporated brines, several per mil heavier than normal seawater (e.g., modern Arabian Gulf water in the range of 2.5 to 4‰ [Wood et al., 2002])
- Using a similar enrichment over Mississippian seawater values gives a potential fluid for dolomitization in the range of 0.5 to 3‰
- Coupled with Leadville dolomite values, dolomitization temperatures are constrained to around 60-90°C